

Predicting Stereoscopic Viewing Comfort Using a Coherence-Based Computational Model

Christian Richardt Lech Świrski Ian P. Davies Neil A. Dodgson

Computer Laboratory, University of Cambridge, United Kingdom

Abstract

We introduce a novel computational model for objectively assessing the visual comfort of stereoscopic 3D imagery. Our model integrates research in visual perception with tools from stereo computer vision to quantify the degree of stereo coherence between both stereo half-images. We show that the coherence scores computed by our model strongly correlate with human comfort ratings using a perceptual study of 20 participants rating 80 images each. Based on our experiments, we further propose a taxonomy of stereo coherence issues which affect viewing comfort, and propose a set of computational tools that extend our model to identify and localise stereo coherence issues from stereoscopic 3D images.

Categories and Subject Descriptors (according to ACM CCS): I.2.10 [Artificial Intelligence]: Vision and Scene Understanding—Perceptual reasoning; I.4.8 [Image Processing]: Scene Analysis—Depth cues & stereo

1. Introduction

We investigate how differences between the left and right stereo half-images cause varying types and levels of visual discomfort. We were motivated to study this by considering how to generalise non-photorealistic filters to stereoscopic imagery. We applied over fifty different non-photorealistic effects to a range of stereo images and observed that the visual artefacts fell into three broad categories:

- **binocular rivalry**: noticeably different object boundaries or image content in the two half-images;
- **the shower door effect**: identical texture composited into both half-images; and
- **randomness**: noise and procedurally generated textures.

These artefacts all generate visual discomfort.

Our three-way categorisation was produced by subjective observation by expert viewers. We next considered whether a deterministic algorithm could be produced that would correlate well with subjective observations.

The main contribution of this paper is a computational model that assesses the coherence of stereo half-images and predicts comfort levels from stereoscopic 3D images. Our model is based on recent work in visual perception [BGL04, FB09], which showed similarities between human

observers and normalised cross-correlation [Han74, Sze10] – a local stereo correspondence technique.

We validated our computational model using a perceptual study, in which we showed 80 stereo images to 20 observers and asked them to rate their level of comfort for each image. The results show that our model performs on a par with human observers. Our computational model could therefore be used to automatically assess the visual comfort levels of stereoscopic imagery, without the need to run costly perceptual studies.

In addition to this computational model, we developed a set of extensions that automatically identify and localise coherence issues in stereoscopic 3D imagery.

2. Related Work

Interest in stereoscopic 3D imagery has seen a resurgence in recent years. This development has been primarily driven by the film industry, which has taken advantage of the availability of improved stereoscopic 3D projection technology. However, even the latest stereoscopic 3D displays can lead to visual discomfort and fatigue [LIFH09, How11] for a variety of reasons related to the physiology of vision:

- **vergence–accommodation conflicts**, caused by the need to focus on the screen instead of the virtual point in 3D space [HGAB08];

- **lack of focus cues**, usually caused by defocus blur away from the plane of fixation [HGAB08];
- **absence of motion parallax**, caused because moving the head does not change the images viewed by the two eyes [How11];
- **variance of inter-pupillary distance (IPD)**, caused when the assumed IPD does not match that of the viewer – no single IPD will be right for all people [Dod04];
- **excessive screen disparity**, caused when objects are pulled too far out of the screen, or pushed back “beyond infinity” – this prevents binocular fusion and leads to diplopia (double vision) [LIFH09];
- **crosstalk**, caused by optically imperfect separation of stereoscopic views which results in ‘ghost images’ [SMIO5]; and
- **discrepancy between the images**, caused by a range of effects, including blur, vertical disparity, image compression, and the application of some non-photorealistic filters to the imagery [KT04, BLCCC08].

This work is, obviously, concerned with the last of these.

Kooi and Toet [KT04] were the first to experimentally analyse the effect that different image manipulations have on stereoscopic viewing comfort. They considered 35 different image manipulations, including spatial distortions, crosstalk, blur, luminance and contrast adjustments. Based on their experimental results, they concluded that vertical disparity, crosstalk and blur were the factors that most strongly determined visual discomfort. However, the authors’ primary contribution was to provide the experimental basis for systems that predict the viewing comfort of stereoscopic display systems. While we do not use their data, we propose such a system to objectively measure viewing comfort.

Stavrakis and Gelautz [SG05] described the problems in creating stereoscopic artwork and outlined strategies for extending ‘monocular’ NPR techniques to stereo 3D. Our work expands on their ‘consistency’ and ‘randomness’ criteria.

Benoit et al. [BLCCC08] proposed a stereoscopic image quality assessment metric for assessing the impact of image compression like JPEG and JPEG2000 on the stereoscopic viewing experience. In their metric, they combine conventional image metrics (SSIM, C4) applied to each half-image with a disparity distortion measure, which encodes the difference between the disparity maps of the original and distorted stereo images. Like all image quality metrics, their work relies on the original stereo image being available, whereas our model does not. For computing disparity maps, they use state-of-the-art stereo matching techniques like belief propagation and graph cuts [SS02], while we use the simpler normalised cross-correlation technique. The latter has been shown to have performance similar to that of humans in a number of psychovisual experiments [BGL04, FB09, VFB09].

3. Taxonomy of Stereo Coherence Issues

We began our work with the question: Which categories of image manipulations are most detrimental to visual comfort?

In a pilot study, two of the authors viewed all combinations of six stereo images and 51 Photoshop filters – a total of 306 manipulated images. During this process, they took free-form notes on all images and later independently categorised the issues they perceived into as many groups as seemed appropriate.

The categories produced independently by the two authors were nearly identical. We combined them into a taxonomy that we believe represents the major stereo coherence issues in this dataset: binocular rivalry, the shower door effect, and randomness. These categories, which can overlap to some degree, are illustrated by example in figure 1, and we define and describe them in more detail in the following sections.

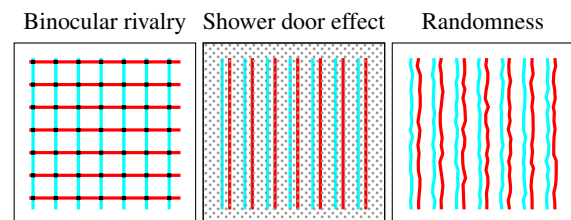



Figure 1: Anaglyph  examples of the three categories of stereo coherence issues that we identified in our taxonomy. The red-cyan anaglyph images in this paper are best viewed at a larger zoom level on a computer display.

3.1. Binocular Rivalry

Binocular rivalry, also known as retinal rivalry, describes the alternations in perception that are experienced when mismatched stimuli are presented to the two eyes [Bla01, BL02]. The first detailed description of this phenomenon is due to Wheatstone [Whe38], who mounted different letters in his stereoscope and described his observations. What he saw was that one eye’s stimulus dominates over the other for a few seconds, until the image “breaks into fragments, while fragments of the letter which is about to appear mingle with them, and are immediately after replaced by the entire letter”, and that this process would repeat every few seconds.

Binocular rivalry is caused whenever image regions are strongly conflicting between the two stereo half-images, that is if they are not in correspondence with a region in the other half-image. This definition has some overlap with our third category, randomness, so we restrict our definition to regions covering at least a few degrees of visual arc. We identified rivalry issues in Photoshop filters that use morphological operators, segmentation and colour quantisation, as they can modify object boundaries or even remove them completely. For an example, please refer to figure 6 in section 7.1.

3.2. Shower Door Effect

The ‘shower door effect’ is a term that is commonly used in non-photorealistic rendering [GG01] to describe a look that resembles textured glass in front of the main content of an image. This effect is most easily achieved by compositing identical textures into both stereo half-images, like in the ‘texturizer’ filter shown in figure 2. The resulting flat, transparent texture has a disparity of zero, which places it exactly on the screen. If it is in front of other objects then it creates a visible artefact in the plane of the screen, which distorts what is behind it [AT88]. If it is behind other objects, the situation is worse because there are conflicting stereo cues: the ‘shower door’ appears to be in front of the objects visually but behind them in terms of depth. This conflict increases visual discomfort.

Another, perhaps more deserving example is the ‘glass’ effect in figure 2, which applies an identical distortion to both half-images. The result looks like a shower door with rippled glass, or, “like looking through a window”, as one of our study participants put it.

3.3. Randomness

Our final category captures everything where randomness is in play. In general, if the same effect applied twice to an image produces two noticeably different resulting images, then the stereo half-images are also most likely incoherent. The simplest example is per-pixel noise, such as film grain. While small amounts of noise are tolerated by the human visual system, stronger noise in the half-images can make it hard to fuse them, which causes visual discomfort. Another example is the ‘chalk & charcoal’ effect in figure 2, which places strokes randomly and with random length.

One way to ameliorate the effects of randomness is to fix the seed value of the random number generator. In general, this reduces to the shower door effect of the previous section, as the same manipulation is now applied to both half-images. One example of this is the ‘ocean ripple’ filter in figure 2, which would produce results resembling the ‘glass’ filter, which we found had higher viewing comfort (see section 6).

4. Computational Model

The primary aim of our paper is to provide a computational model for objectively estimating the level of visual comfort from a given stereoscopic 3D image. In our model, we combine research in visual perception [FB09] with tools from stereo computer vision [EW02] to construct a metric for visual comfort based on stereo coherence – that is, the consistency of the two stereo half-images.

The input to our computational model is the pair of stereo half-images and the range of disparities used in the image. The output is a coherence score, i.e. the percentage of consistent pixels, which we found to be a good indicator for visual comfort (see sections 5 and 6).

Our model is based on a computational model of human stereopsis – depth perception from binocular disparity – recently proposed by Filippini and Banks [FB09]. As per their model, the left and right images are first blurred according to the optical properties of the human eye (section 4.1). We then use their local cross-correlator (section 4.2) to compute disparity maps for the two half-images. In the last step, we apply the left-right consistency check [EW02] to check if corresponding pixels in both disparity maps have consistent disparities (section 4.3).

We show results of our model in section 4.4, but leave the full experimental validation of our model to section 6. In section 7, we further propose a set of computational tools extending our model to identify and localise stereo coherence issues.

4.1. Optical Blur of the Human Eye

The first step in our computational model is a preprocess that applies a mixture of two isotropic 2D Gaussian blurs to the stereo half-images, in order to emulate the optical properties of the human eye. Specifically, we apply the point-spread function of the well-focused eye with a 3 mm pupil after Geisler and Davila [GD85]:

$$h(x, y) = a \cdot g_{s_1}(x, y) + (1 - a) \cdot g_{s_2}(x, y), \quad (1)$$

where the 2D Gaussian blur of standard deviation s is

$$g_s(x, y) = (2\pi s^2)^{-1} \cdot e^{-(x^2+y^2)/2s^2}, \quad (2)$$

with $a = 0.583$, $s_1 = 0.433$ arcmin, and $s_2 = 2.04$ arcmin. This set of parameters assumes that the distance between pixels, and therefore the pixel size, is 0.6 arcmin, which roughly corresponds to the spacing between foveal cones.

4.2. Local Cross-Correlator

Banks et al. [BGL04] first introduced local cross-correlation as a computational model to help explain why spatial stereo-resolution is lower than luminance resolution. The technique they used is known as normalised cross-correlation in the computer vision literature [SS02], and it works by calculating the correlation between windows of pixels in both stereo half-images. The correlation between windows of disparity d is given by

$$c(d) = \frac{\sum_{(x,y) \in W} (L(x,y) - \mu_L)(R(x-d,y) - \mu_R)}{\sqrt{\sum_{(x,y) \in W} (L(x,y) - \mu_L)^2} \sqrt{\sum_{(x,y) \in W} (R(x-d,y) - \mu_R)^2}}, \quad (3)$$

where L and R are the intensities of the left and right images, and μ_L and μ_R are the mean intensities within the windows.

In Banks et al.’s original version [BGL04], the correlation window W is a square, but Filippini and Banks [FB09] recently proposed to mimic the envelopes associated with

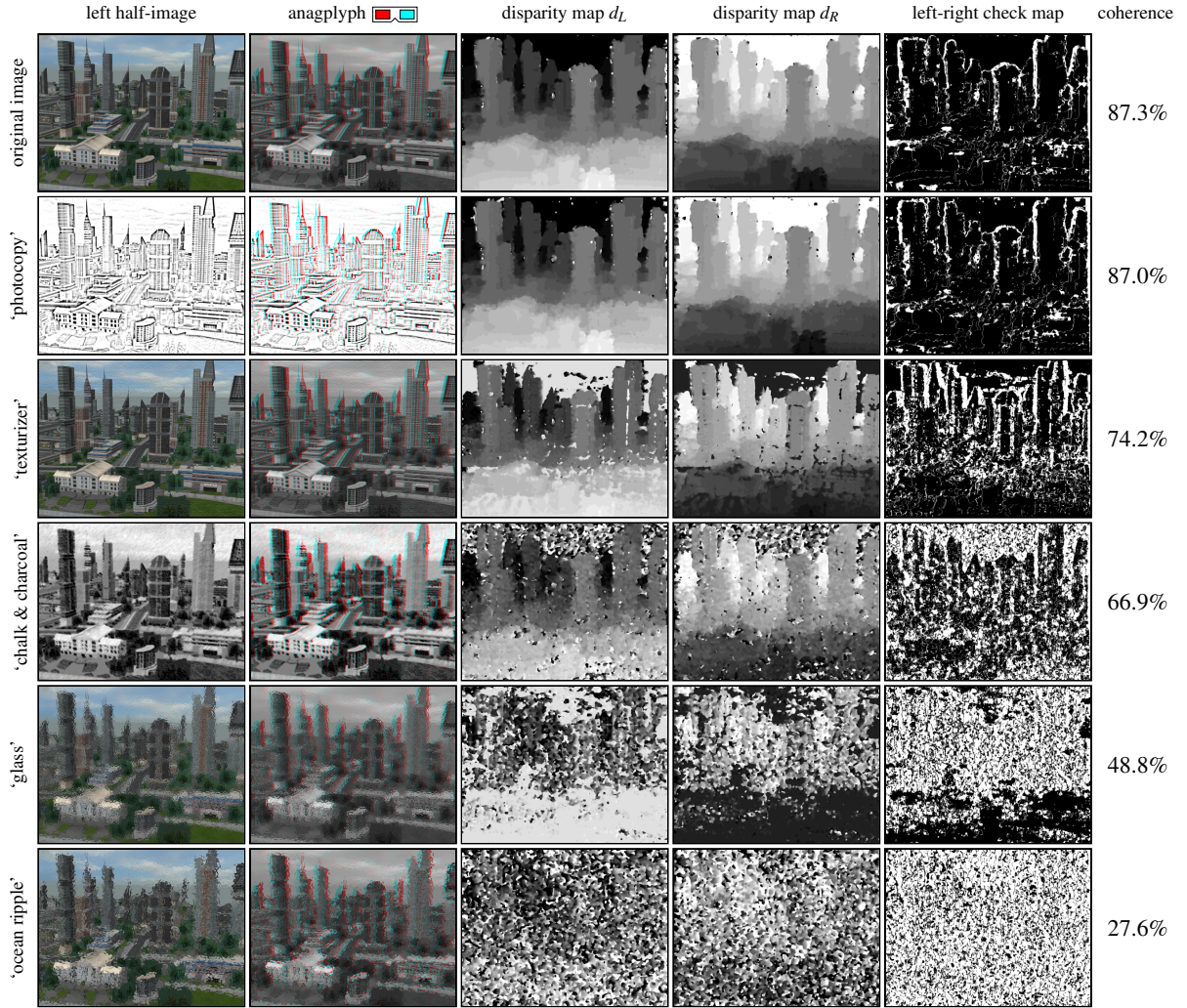


Figure 2: Results of our computational model on the ‘city’ stereo image and five versions manipulated using Photoshop filters. The disparity maps d_L and d_R , which are scaled to the visible range, are near-inverses of each other, and as filters produce less coherent results, the disparity maps get noisier and more inconsistent as measured using the left-right check. The coherence score in the last column is the percentage of consistent (black) pixels in the left-right check map. Please zoom in for details.

cortical receptive fields using a Gaussian weighting function (truncated at 3σ):

$$W = e^{-(x^2+y^2) / 2\sigma^2}. \quad (4)$$

Filippini and Banks report the best results for $\sigma = 3$ arcmin, which corresponds to 5 pixels, as per the assumptions above.

We compute disparity maps using winner-take-all [SS02], by selecting the disparity with the highest correlation score:

$$d_L(x,y) = \arg \max_{d \in D} c(d). \quad (5)$$

4.3. Left-Right Check (LRC)

The left-right consistency check is a popular technique in stereo matching for identifying occluded or otherwise inconsistent pixels in disparity maps [EW02]. The check works on two disparity maps: the left-to-right disparity map $d_L(x,y)$ and the right-to-left disparity map $d_R(x,y)$. Since both disparity maps are for roughly the same view, they should be ‘inverses’ of each other, and the disparities of corresponding pixels should sum to zero. A pixel $d_L(x,y)$ in the left-to-right disparity map is hence considered consistent if this sum falls below a threshold T_{LRC} (we use $T_{LRC} = 1$ throughout):

$$\left| d_L(x,y) + d_R(x - d_L(x,y), y) \right| < T_{LRC}. \quad (6)$$

4.4. Results

Figure 2 shows results of our computational model applied to the computer-generated stereo image of a city as well as five versions of it with Photoshop filters applied to the left and right half-images independently. As the stereo images get increasingly incoherent, the coherence score computed by our model decreases steadily. It is interesting to note that the original image does not achieve a perfect coherence score according to our model, which is caused by errors in the stereo matching as well as occlusions in the half-images. Please see section 6 for a full experimental validation of our model using subjective human ratings of visual comfort.

5. Perceptual Study

In order to validate our computational model, we conducted a perceptual study in which we asked volunteers to rate the viewing comfort of 80 stereo images. Our hypothesis was that there would be a strong correlation between human comfort ratings and the coherence score produced by our model, which would indicate that we are able to automatically assess the visual comfort levels of stereoscopic images with performance similar to that of human observers. The hypothesis was confirmed by the results of the experiment, as detailed and discussed in section 6.

5.1. Experimental Setup

We recruited 20 participants (12 male and 8 female) between the ages of 20 and 60. All had normal or corrected-to-normal vision and none reported any problems with stereopsis.

Figure 3 shows our experimental setup. Stereoscopic 3D images were displayed using a DepthQ projector by Light-speed Design Inc. and were viewed through passive polarising glasses from two chairs placed side-by-side in the centre of the room.

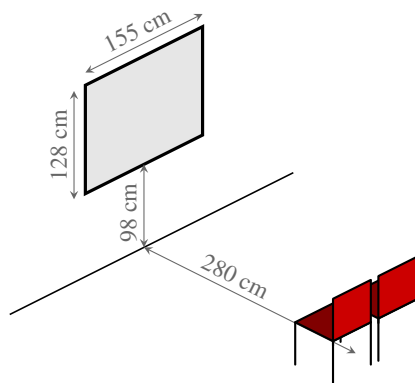


Figure 3: Experimental setup.

5.2. Stimuli

A pilot study was conducted in which we considered all combinations of six stereo images with 51 Photoshop filters. Three of the images were self-generated and three were from the Middlebury stereo datasets [SS03]. To design an experiment that could be completed in reasonable time, we selected a subset of the 306 images which covered the full range of artefacts described in section 3. We chose 4 images (figure 4) and 19 filters (table 1) for a total of 80 images (including the originals) to be rated by the participants.

We rescaled all the images to the projector's height of 720 pixels, and adjusted horizontal disparity by shifting so that the front-most object was just in front of the screen, to ease viewing by avoiding excessive disparities.

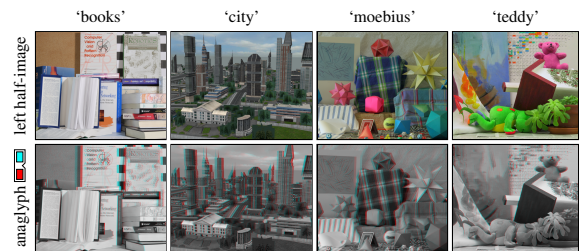


Figure 4: The four original stereo images used in our study.

Chalk & Charcoal	Halftone Pattern	Rough Pastels
Craquelure	Ocean Ripple	Spatter
Cutout	Paint Daubs	Stained Glass
Diffuse Glow	Palette Knife	Stamp
Find Edges	Photocopy	Texturizer
Glass	Poster Edges	
Grain	Reticulation	

Table 1: The 19 Photoshop filters used in our study.

5.3. Procedure

Participants were asked to rate each of the 80 images for viewing comfort on a five-point Likert scale ranging from 1 (very uncomfortable) to 5 (completely comfortable) and we clearly explained that they were being asked to rate physical comfort rather than any aesthetic quality of the images. Participants were scheduled to complete the experiment in pairs to save time; no discussion was allowed. For each pair the order of the images was randomised for counter-balancing.

Before beginning the main experiment, ten additional images were shown to allow the participants to familiarise themselves with the experimental environment. Participants were given as long as they wanted to rate each image and were allowed to change their minds until they were content with each rating. Each experimental run took around 15 minutes to complete.

6. Experimental Validation

The perceptual study of the previous section produced 1600 user ratings – 20 ratings each for the 80 stereo images that were shown. Our computational model also produces a rating for each of the images, albeit a coherence score in the range from 0 to 100%, whereas the user ratings are given on a five-point Likert scale from 1 to 5.

Because of this difference in scale, we analyse similarities between user ratings and our model using correlation coefficients. Specifically, we use Spearman’s rank correlation coefficient, as we assume the relationship between ratings to be monotonic but not necessarily linear. Table 2 summarises the distribution of correlation coefficients between pairs of users, the average user rating for each image, as well as our computational model.

The top half of table 2 shows that the correlation between our model and any user is close to the correlation between pairs of users. From this we conclude that our model’s scores are as good a fit to users’ ratings as any other user’s ratings. In the bottom half of table 2, we compare user and model ratings to the average user rating for each image across all 20 users. The bottom row only shows a single correlation coefficient, and not a distribution of them. Our model is a good fit to the mean user rating for the first quartile, but it is less correlated above it. Nevertheless, our computational model is strongly correlated with the average user ratings.

To bring our model’s score into the same range as the user ratings, we rescale it linearly using a least squares fit:

$$x' = 4.36 \cdot x - 0.07, \quad (7)$$

which achieves a root mean square error (RMSE) of 0.59. The absolute term is close to zero, which suggests a direct relationship between stereo coherence and visual comfort.

The remaining differences in the average and predicted user ratings are shown as a histogram in figure 5. Our model predicts 70 out of 80 images (88 percent) to within a unit of comfort – the baseline is 46 percent for uniformly distributed scores and 56 percent for always scoring a ‘3’. The images near the negative end of the axis, where our model underes-

	mean	quartiles				
		0%	25%	50%	75%	100%
user – user	0.69	0.46	0.63	0.70	0.75	0.85
user – model	0.69	0.48	0.67	0.71	0.73	0.79
mean – user	0.83	0.68	0.80	0.84	0.87	0.91
mean – model	0.81	—	—	—	—	—

Table 2: Distribution of Spearman’s correlation coefficients between pairs of users, the mean user rating and our computational model. Please see section 6 for discussion.

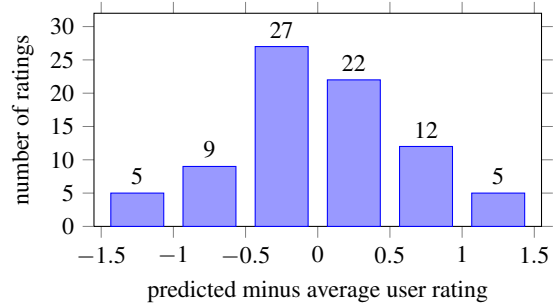


Figure 5: The histogram of differences between the ratings predicted by our model and the average user rating (our model overestimates visual comfort for positive differences).

timates visual comfort by more than one unit, are caused by noise, which the human visual system is good at filtering out, and by the limitation that our model cannot produce a perfect correlation score, as mentioned in section 4.4. The outliers where our system overestimates visual comfort are mostly caused by the ‘shower door effect’ (see section 3.2), which our model appears to tolerate better than human observers.

Our setup (figure 3) has a pixel size of 2.2 arcmin compared to the 0.6 arcmin assumed in our model. However, we found that assuming a pixel size of 0.6 arcmin in our model resulted in a higher correlation to user ratings (0.81 vs 0.67) as well as reduced noise in the disparity maps.

In summary, we conclude that our computational model is a good predictor of stereoscopic viewing comfort. It correlates strongly with comfort ratings given by human observers, and 88 percent of predicted comfort ratings are to within one unit of comfort to the average user rating.

7. Computational Tools for Stereo Coherence Analysis

Our computational model is based on the general approach of checking disparity maps for consistency. This allows our model to objectively quantify the degree of stereo coherence, and thus estimate viewing comfort. However, because of this generality, our model cannot differentiate between different types of incoherencies, which would be of interest to content creators such as artists. For this purpose, we propose extensions to our computational model that help to identify and localise stereo coherence issues.

7.1. Binocular Rivalry

The left-right consistency map created by our computational model highlights inconsistencies between the half-images directly. To reduce the influence of occlusion artefacts, we further apply a 2D Gaussian blur with the same parameters used in windowing the local cross-correlator of section 4.2. This is because the human visual system does not operate on a ‘per-pixel’ level, but rather using larger receptive fields. Some results of this approach are shown in figure 6.

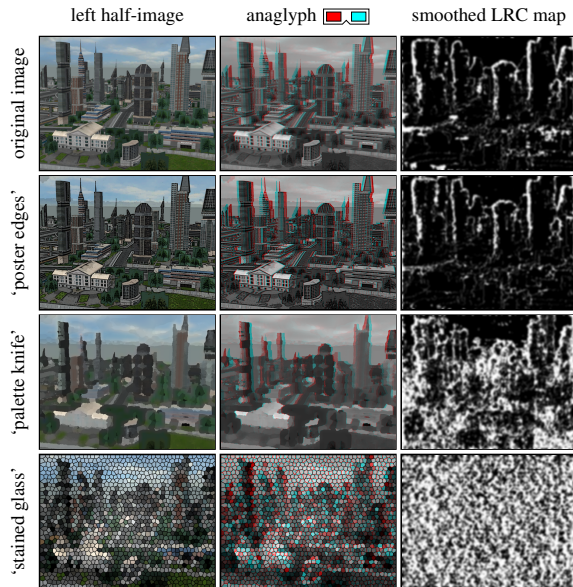


Figure 6: Examples of our binocular rivalry detection (see section 7.1): the ‘poster edges’ effect causes hardly any binocular rivalry, ‘palette knife’ shows artefacts near object boundaries, and ‘stained glass’ is globally incoherent.

7.2. Shower Door Effect

The coherence analysis concentrates on issues which involve binocular rivalry. However, in the shower door effect, there are no rivalry issues, but the 3D structure perceived due to stereopsis may be ambiguous or incorrect [AT88]. The normalised cross-correlator (section 4.2) can be used to detect these issues. Recall that it computes a pixel’s most likely disparity as the one which has the globally maximal correlation over all disparities.

We extend this to define a pixel’s ‘likely disparities’ as those with locally maximal correlations. In the shower door effect, an identical texture is blended onto both stereo half-images, with zero disparity. Given the blending, this texture’s zero disparity may not be the most likely disparity, and therefore would be discarded when using the winner-takes-all approach. However, it may still be a likely disparity; the shower door effect can hence be detected as a large number of pixels having a likely zero disparity.

For detecting the shower door effect, we use an approach inspired by the Hough transform [DH72]. Where the Hough transform detects linear image structure by accumulating possible lines, we use an accumulator to detect likely disparities; in particular, we accumulate likely disparities over all pixels, creating a histogram of the frequency of likelihood for each disparity. With this definition, peaks in the accumulator correspond to many pixels having the same likely disparity. A strong peak at zero disparity is indicative of the shower door effect, as shown in figure 7.

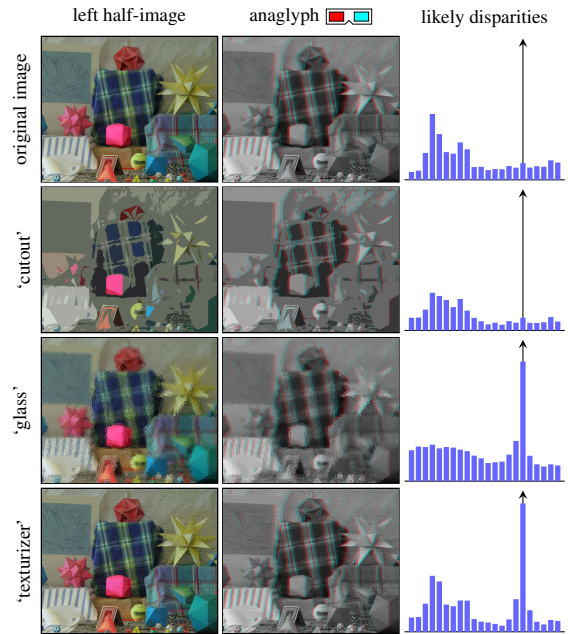


Figure 7: Results of our ‘shower door effect’ detection (see section 7.2). Notice that the bottom two effects have large peaks at a likely disparity of zero (at the upwards pointing y-axis), which is indicative of the shower door effect.

7.3. Randomness

An elementary check for randomness in a particular filter (see section 3.3) is to apply the filter twice to the same image and to compare the resulting images. This comparison can also be automated using image quality metrics such as peak signal-to-noise ratio (PSNR) or structural similarity (SSIM).

However, it is not always possible to apply an effect twice, for example when working with existing stereo imagery. Also, it may be the case that the effect is pseudo-random, seeded by the image data. Then, the ‘noise’ will be the same regardless of how many times the effect is applied; however, it may look vastly different if applied to the two slightly different stereo half-images.

For both of these cases, we propose an image-based cross-check built on our computational model, which is also capable of indicating problem areas. For all pixels that are indicated as consistent by the left-right check map (section 4.3), we look up their corresponding colours in the half-images, and compute the ΔE_{ab}^* colour difference between them in the CIELAB colour space. Pixels with inconsistent disparities are set to zero. As before, we then apply a 2D Gaussian blur to mimic the behaviour of receptive fields.

The result is that images with correctly calculated disparity but rivalry due to noise can easily be detected as having a mostly white image cross-check, as shown in figure 8.

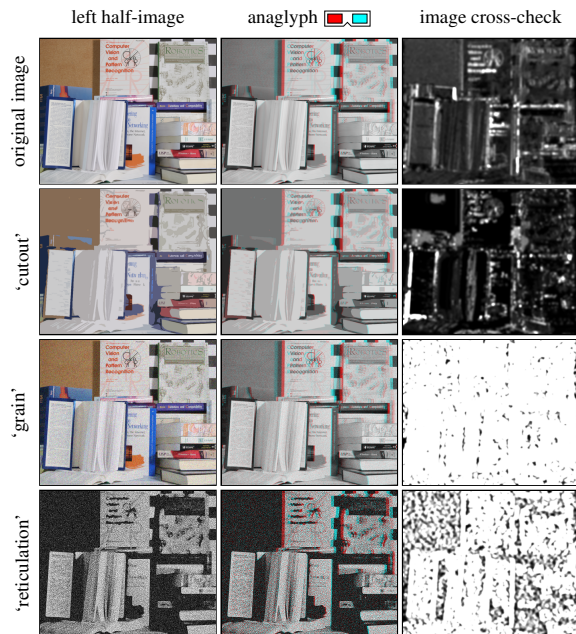


Figure 8: Results of our image-based cross-check (section 7.3). The bottom two filters show a lot of randomness.

8. Conclusion

We proposed the first computational model for predicting the viewing comfort of stereoscopic 3D images. Our model is based on research in visual perception, and we showed that it strongly correlates with human comfort ratings. This makes our model ideal for automatically assessing stereoscopic 3D content without the need for costly and lengthy perceptual studies. We also introduced a taxonomy of stereo coherence issues and demonstrated how our model can be extended to detect and localise such issues.

Future work could improve the performance of our model even further. Firstly, improved occlusion handling would allow a more accurate comfort prediction for coherent stereo images. And secondly, global stereo matching techniques would improve handling of weakly textured areas. An interesting orthogonal direction of future work is the analysis of stereo-temporal coherence in time-varying stereoscopic 3D imagery.

References

- [AT88] AKERSTROM R., TODD J.: The perception of stereoscopic transparency. *Attention, Perception & Psychophysics* 44, 5 (September 1988), 421–432. 3, 7
- [BGL04] BANKS M., GEPSHTEIN S., LANDY M.: Why is spatial stereoresolution so low? *Journal of Neuroscience* 24, 9 (March 2004), 2077–2089. 1, 2, 3
- [BL02] BLAKE R., LOGOTHETIS N. K.: Visual competition. *Nature Reviews Neuroscience* 3, 1 (January 2002), 13–21. 2
- [Bla01] BLAKE R.: A primer on binocular rivalry, including current controversies. *Brain and Mind* 2, 1 (April 2001), 5–38. 2

- [BLCCC08] BENOIT A., LE CALLET P., CAMPISI P., COUSSEAU R.: Quality assessment of stereoscopic images. *EURASIP Journal on Image and Video Processing* 2008 (2008), 659024:1–13. 2
- [DH72] DUDA R. O., HART P. E.: Use of the Hough transformation to detect lines and curves in pictures. *Communications of the ACM* 15, 1 (January 1972), 11–15. 7
- [Dod04] DODGSON N. A.: Variation and extrema of human interpupillary distance. In *Stereoscopic Displays and Virtual Reality Systems* (January 2004), vol. 5291 of *Proceedings of SPIE*. 2
- [EW02] EGNAL G., WILDES R. P.: Detecting binocular half-occlusions: Empirical comparisons of five approaches. *IEEE Transactions on Pattern Analysis and Machine Intelligence* 24, 8 (August 2002), 1127–1133. 3, 4
- [FB09] FILIPPINI H. R., BANKS M. S.: Limits of stereopsis explained by local cross-correlation. *Journal of Vision* 9, 1 (January 2009), 8:1–18. 1, 2, 3
- [GD85] GEISLER W. S., DAVILA K. D.: Ideal discriminators in spatial vision: two-point stimuli. *Journal of the Optical Society of America A: Optics and Image Science* 2, 9 (September 1985), 1483–1497. 3
- [GG01] GOOCH B., GOOCH A.: *Non-Photorealistic Rendering*. A K Peters, 2001. 3
- [Han74] HANNAH M. J.: *Computer Matching of Areas in Stereo Images*. PhD thesis, Stanford University, 1974. 1
- [HGAB08] HOFFMAN D., GIRSHICK A., AKELEY K., BANKS M.: Vergence-accommodation conflicts hinder visual performance and cause visual fatigue. *Journal of Vision* 8, 3 (March 2008), 1–30. 1, 2
- [How11] HOWARTH P. A.: Potential hazards of viewing 3-D stereoscopic television, cinema and computer games: a review. *Ophthalmic and Physiological Optics* 31, 2 (February 2011), 111–122. 1, 2
- [KT04] KOOI F. L., TOET A.: Visual comfort of binocular and 3D displays. *Displays* 25, 2–3 (August 2004), 99–108. 2
- [LIFH09] LAMBOOIJ M., IJSELSTEIJN W., FORTUIN M., HEYNDERICKX I.: Visual discomfort and visual fatigue of stereoscopic displays: A review. *Journal of Imaging Science and Technology* 53, 3 (May/June 2009), 030201:1–14. 1, 2
- [SG05] STAVRAKIS E., GELAUTZ M.: Computer generated stereoscopic artwork. In *Computational Aesthetics* (May 2005). 2
- [SMI05] SEUNTIENS P. J. H., MEESTERS L. M. J., IJSELSTEIJN W. A.: Perceptual attributes of crosstalk in 3D images. *Displays* 26, 4–5 (October 2005), 177–183. 2
- [SS02] SCHARSTEIN D., SZELISKI R.: A taxonomy and evaluation of dense two-frame stereo correspondence algorithms. *International Journal of Computer Vision* 47, 1–3 (April 2002), 7–42. 2, 3, 4
- [SS03] SCHARSTEIN D., SZELISKI R.: High-accuracy stereo depth maps using structured light. In *Proceedings of the International Conference on Computer Vision and Pattern Recognition (CVPR)* (June 2003), pp. 195–202. 5
- [Sze10] SZELISKI R.: *Computer Vision: Algorithms and Applications*. Springer, 2010. 1
- [VFB09] VLASKAMP B. N. S., FILIPPINI H. R., BANKS M. S.: Image-size differences worsen stereopsis independent of eye position. *Journal of Vision* 9, 2 (February 2009), 17:1–13. 2
- [Whe38] WHEATSTONE C.: Contributions to the physiology of vision.—Part the first. On some remarkable, and hitherto unobserved, phenomena of binocular vision. *Philosophical Transactions of the Royal Society of London* 128 (1838), 371–394. 2